Tungsten Disulfide-reduced GO/CNT Aerogel: A Tuned Interlayer Spacing Anode for Efficient Water Desalination

Sareh Vafakhah [a], Mohsen Saeedikhani [b], Shaozhuan Huang [c], Dong Yan [a], Zhi Yi Leong [a], Ye Wang [d], Lijuan Hou [d], Lu Guo [a, *], Pablo Valdivia y Alvarado [a], Hui Ying Yang [a, *]

[a] Pillar of Engineering Product Development, Singapore University of Technology and Design, Singapore 487372

[b] Department of Materials Science and Engineering, National University of Singapore, 9 Engineering Drive 1, Singapore 117576

[c] Key Laboratory of Catalysis and Energy Materials Chemistry of Ministry of Education, South-Central University for Nationalities, Wuhan, Hubei, 430074, China

[d] Key Laboratory of Material Physics, Ministry of Education, School of Physics and Microelectronics, Zhengzhou University, Zhengzhou, 450052, China

[*]Corresponding Author

Email: yanghuiying@sutd.edu.sg, lu_guo@sutd.edu.sg

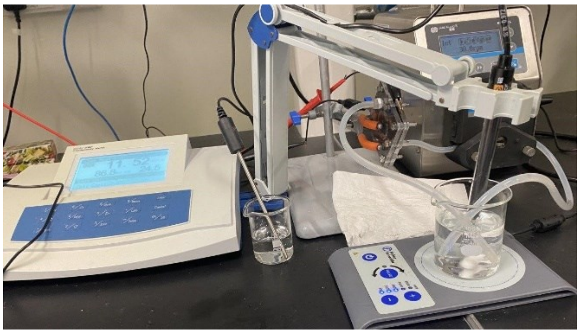

Figure S1, photograph of HCDI set up.

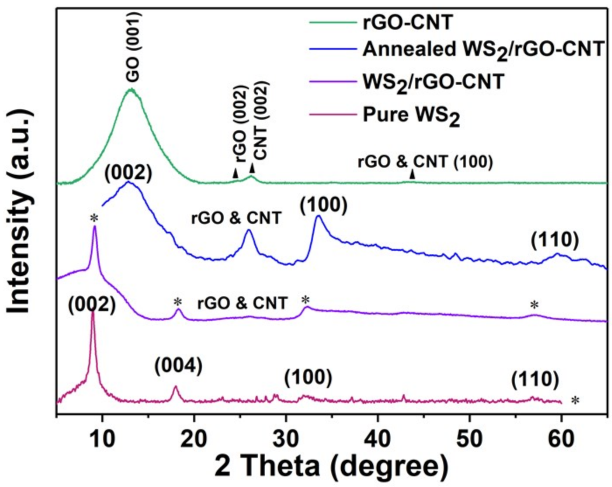

Figure S2, XRD pattern of rGO-CNT.

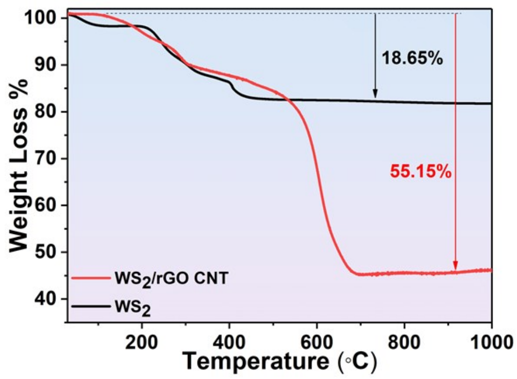

Figure S3, TGA analysis to determine the amount of WS_2 in WS_2/rGO-CNT composite

In order to calculate the percentage of WS_2 and rGO-CNT in the composite, TGA experiments were performed for both WS_2/rGO-CNT aerogel and pure WS2 as a reference sample. Therefore, the WS_2 content can be calculated using below equation, meaning the residual amount for both samples at 800 °C have the same compositions:

$$\frac{(1 - 18.65\ \%)wt\%_{\ WS2}}{wt\%_{rGO\ -\ CNT} + wt\%_{\ WS2}} = (1 - 55.15\%)$$

$$wt\%_{WS2} = 55.13\%$$

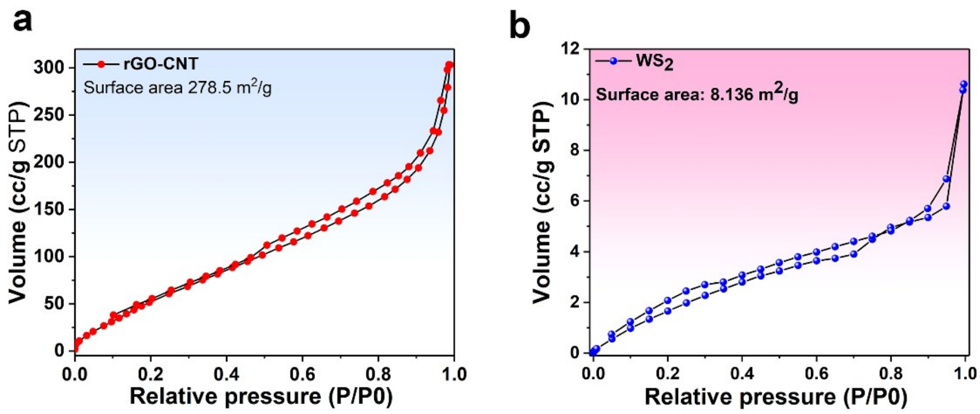

Figure S4, BET nitrogen adsorption-desorption isotherm, a) of rGO-CNT, and b) pure WS_2 powder.

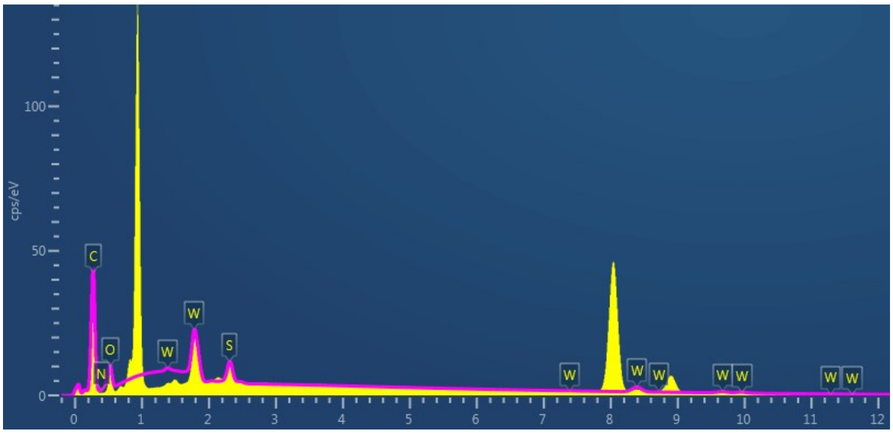

Figure S5, the elemental analysis of WS_2/rGO-CNT with EDS, indicating the atomic ratio of W to S as ~ 1:1.7 (0.3 atomic positions are occupied with oxygen content). The excess peaks are related to the cupper substrate.

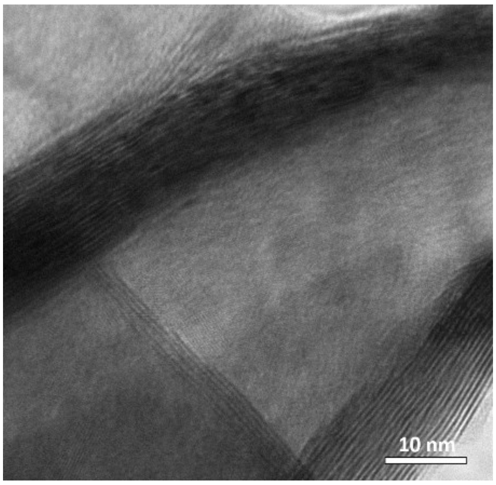

Figure S6, the HRTEM image for annealed WS_2/rGO-CNT indicating the interlayer spacing of 0.62 nm between (002) planes.

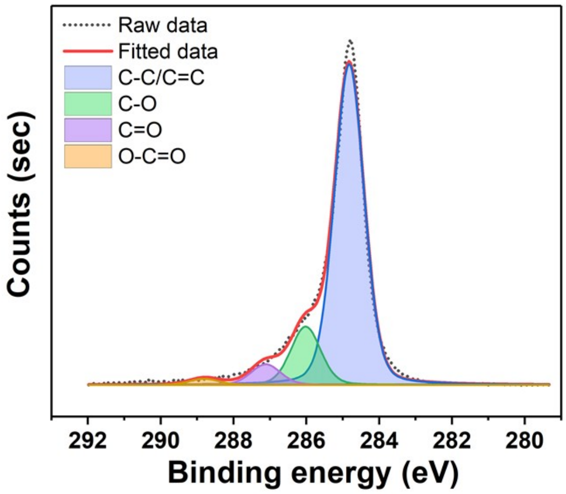

Figure S7, The C1s spectra for nonannealed WS_2/rGO-CNT.

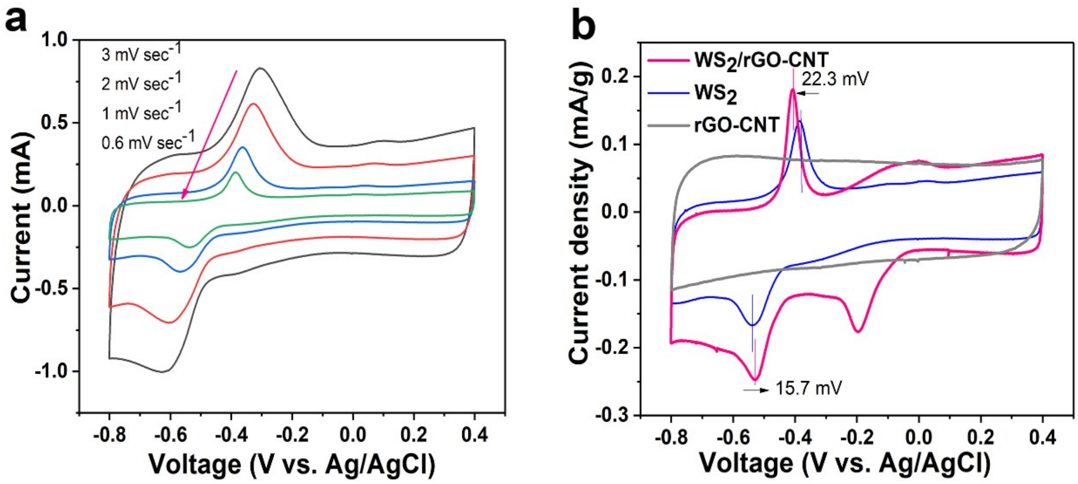

Figure S8, a) the Cyclic voltammetry of pure WS_2 at different scan rates of 0.6, 1, 2 and 3 mV sec^{-1}, and b) the comparison of pure WS_2, bare rGO-CNT, and WS_2/rGO-CNT at scan rate of 0.6 mV sec^{-1}.

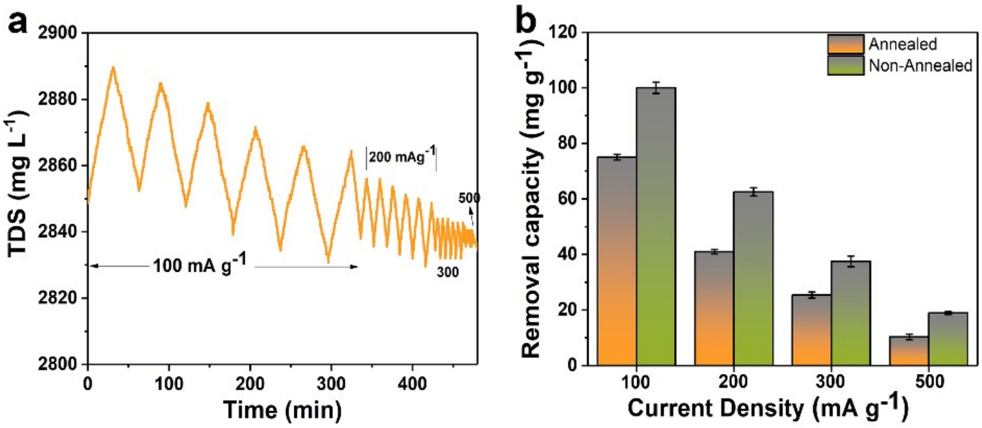

Figure S9, Desalination results for annealed WS_2/rGO-CNT with total mass loading of 20 mg, the voltage range of -1.4 V to 1.4 V and flow rate of 50 mL/min, a) The TDS pattern at different current densities, and b) the comparison of removal capacity between annealed and nonannealed WS_2/rGO-CNT.

Table S1, Desalination performances of recent transition Metal Dichalcogenides (TMDs) applied in CDI systems in comparison with the present work.

Material	CDI mode	Cell vol/Current density	NaCl (mM)	Electrodes mass (mg)	SAC (mg/g)	Energy	Ref
MoS_2/CNT	Symmetric CDI-CV	0-0.8 V/-	500	80-120	25	-	[21]
SnS_2@GP	Symmetric CDI-CV	1.2 V/-	8.5	60	30.32	-	[22]
MoS_2	CDI- CV	1.2 V/-	400		8.81	-	[52]
TiS_2/CNT	HCDI- CV	0.2-0.8 V/-	600	300-330	14	1.2 Wh/L	[20]
MoS_2/GO	MCDI- CV	1.4 V/-	5.13	-	34.2	-	[18]
MoS_2/GO	CDI- CV	1.2 V/-	8.5	-	19.4	-	[19]
WS_2/rGO-CNT	HCDI- CC	1.4 V/25 mA/g	51.3	80	80	55.7 wh/m^3	This work

Table 2, Sodium ion removal results for large scale HCDI device with total electrodes' masses of 80 mg at different current of 10 mA, 3 mA, and 1 mA at synthetic seawater solution with initial concentration of 35 g/L of mixed ions and initial sodium ion concentration of ≈ 8 g/L.

Current (mA)	Salt removal, ΔC (mg/L)	Salt removal percentage (%)	Salt removal capacity (mmol/L)
10	190	2.35	8
3	280	3.62	12
1	580	7	25

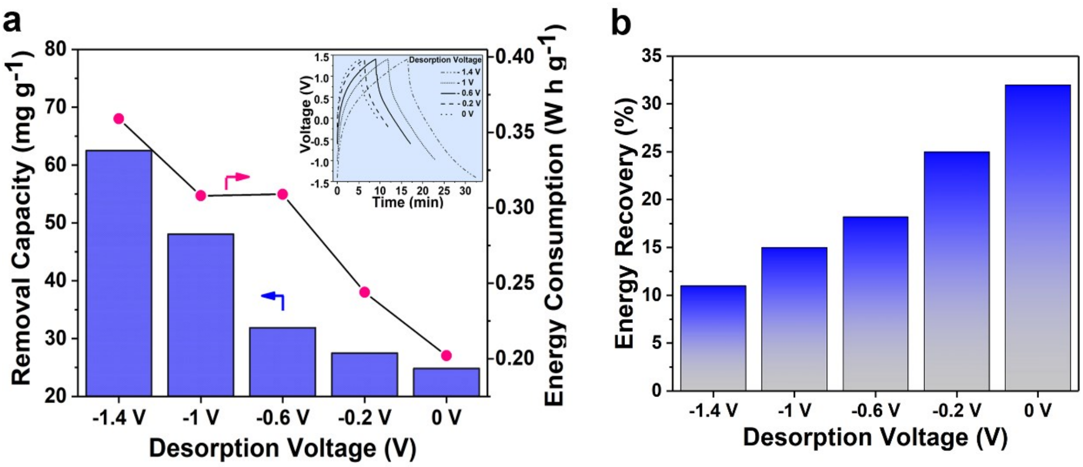

Figure S10, a) The removal capacity and energy consumption, and b) The percentage of energy recovery at different desorption voltages at 200 mA/g.